$^{1}H \rightarrow {}^{31}P$, $^{31}P \rightarrow {}^{1}H$, and $^{2}H \rightarrow {}^{1}H$ CP/MAS NMR Studies of the Large-Pore Gallophosphate Molecular Sieve Cloverite

Waclaw Kolodziejski*,† and Jacek Klinowski*,‡

Faculty of Pharmacy, Department of Inorganic and Analytical Chemistry, Warsaw Medical Academy, ul. Banacha 1, 02-097 Warszawa, Poland, and Department of Chemistry, University of Cambridge, Lensfield Road, Cambridge CB2 1EW, U.K.

Received: October 31, 1996[⊗]

Air-equilibrated cloverite containing normal and deuterated water was studied by ^{1}H, ^{31}P, and ^{71}Ga NMR with magic-angle spinning (MAS). The spectra are assigned, and the ^{1}H and ^{31}P spin−lattice relaxation and the kinetics of $^{1}H \rightarrow {}^{31}P$, $^{31}P \rightarrow {}^{1}H$, and $^{2}H \rightarrow {}^{1}H$ cross-polarization (CP) are examined in detail. Spin diffusion between the observed spins (^{1}H or ^{31}P) has a significant effect on the relative intensities of lines in the CP spectra. The results indicate that cloverite contains water-rich and water-deficient microdomains that contribute separately to the overall spectra. The water-rich microdomains contain defect P−OH groups created by the hydrolysis of the Ga−O−P bonds.

Introduction

The gallophosphate cloverite[1−3] has a cubic structure with the unit cell formula $[Ga_{768}P_{768}O_{2976}(OH)_{192}]\cdot 192RF$ (where RF stands for quinuclidinium fluoride template). This molecular sieve has the largest pore openings and cages (1.3 and 2.9 nm in diameter, respectively) found so far in microporous materials and, in this respect, can only be compared with the recently synthesized aluminophosphate JDF-20, which also has 20 T-atom rings.[4] Cloverite contains structural Ga−OH and P−OH groups (Figure 1), the properties of which are essential to its prospective applications. Solid-state ^{1}H NMR with magic-angle spinning (MAS) offers exciting prospects for obtaining information on its structure and acidity. Unfortunately, the ^{1}H peaks from the template protons[3] obscure the peaks from the Brønsted sites, and the template cannot be removed without a structural collapse of the crystal. On the other hand, ^{31}P MAS NMR spectra are poorly resolved,[2,3,5−8] and their interpretation is still uncertain. We will show that cross-polarization (CP),[9−12] deuteration and ultrahigh-speed MAS are of considerable help in the interpretation of the ^{1}H and ^{31}P NMR spectra of cloverite.

Cross-polarization is normally used to enhance low-intensity solid-state NMR signals from *dilute* spins by the polarization transfer from *abundant* spins.[9] Since the process relies on heteronuclear dipolar coupling between the source and target spins, it proceeds faster and gives higher signal intensity if the spins involved are closer in space. In view of this and for relaxation reasons, peak intensities in the CP spectra are different from the intensities in the conventional Bloch-decay (BD) spectrum. For correct interpretation, it is necessary to vary the "contact time" over which CP is performed.[13,14] Such kinetic experiments enable the calculation of the characteristic time constant T_{CP} from which the distances between the participating nuclei can be estimated. The calculation involves rotating-frame relaxation times $T_{1\rho}$ for both spin species, which are usually obtained from separate measurements.

The direction of magnetization transfer during cross-polarization can be reversed, and both $^{31}P \rightarrow {}^{27}Al$ and $^{27}Al \rightarrow {}^{31}P$ CP experiments have been performed with the aluminophosphate VPI-5.[15,16] Since protons are usually used as the polarization source, CP to protons is known as "reverse cross-polarization". We are interested in reverse $X \rightarrow {}^{1}H$ CP ($X = {}^{27}Al$, ^{13}C, ^{2}H) and we have explored all possible combinations of magnetization transfer: *abundant* → *abundant* ($^{27}Al \rightarrow {}^{1}H$ CP in kaolinite),[17] *dilute* → *dilute* ($^{13}C \rightarrow {}^{1}H$ CP in toluene-solvated fullerene-70),[18,19] and *abundant* → *dilute* ($^{2}H \rightarrow {}^{1}H$ CP in perdeuterated glycine).[20] The aim was to interpret the proton spectra by monitoring protons located close to spins X. The $^{31}P \rightarrow {}^{1}H$ CP experiments have been reported only for two model systems, $CaHPO_4$ and KH_2PO_4,[21] the latter being deuterated in order to dilute the protons. The CP kinetics were not studied. We report here the first $^{31}P \rightarrow {}^{1}H$ CP experiments on a "real" system. Cloverite has been examined at natural isotopic abundance (the "abundant → abundant" case) and the performance of CP in both directions has been considered in detail.

In principle, cross-polarization and spin diffusion should always be discussed together. Spin diffusion, which proceeds through flip-flop spin transitions, relies on homonuclear dipolar interactions[22,23] and can be monitored by solid-state NMR

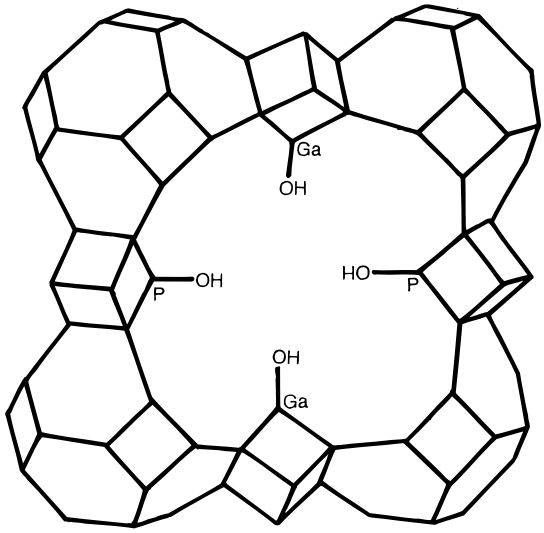

Figure 1. Schematic drawing of the cloverleaf-shaped window to a supercage in the structure of cloverite showing the structural hydroxyl groups pointing into the center of the window. The crossings of straight lines are alternately occupied by Ga and P atoms. Linking oxygen atoms, not shown for clarity, are halfway along the lines.

† Warsaw Medical Academy.
‡ University of Cambridge.
⊗ Abstract published in *Advance ACS Abstracts,* April 15, 1997.

S1089-5647(96)03418-9 CCC: $14.00

TABLE 1: Acquisition Parameters of the Bloch-Decay (BD) and Cross-Polarization (CP) Spectra

	BD			CP		
parameters	^{1}H	^{31}P	^{71}Ga	^{1}H → ^{31}P	^{31}P → ^{1}H	^{2}H → ^{1}H
pulse width (μs)	1.2	1.9	1.1	5.2	5.7	6.0
pulse angle (rad)	$\pi/8$	$\pi/3$	$\pi/10$			
recycle delay (s)	1	20	0.5	1	20	0.5
no. scans	32	32	22 400	120	120	30 000
MAS rate (kHz)	7 or 19	7 or 19	9	7	7	6

experiments in the laboratory[24−26] or rotating[27,28] frames. In a conventional CP experiment it is usually assumed that rapid spin diffusion establishes communication between protons, forcing them to act as a single spin system providing the source of polarization. However, a two-stage CP behavior was observed and explained in terms of insufficiently fast spin diffusion from remote protons to protons directly involved in ^{1}H → ^{13}C CP.[29] On the other hand, during and/or after CP, spin diffusion redistributes magnetization among the target spins. We demonstrate the latter phenomenon for the ^{31}P and ^{1}H spins in cloverite.

Experimental Section

Cloverite was synthesized as follows:[1,2] (1) anhydrous $Ga_2(SO_4)_3$ was dissolved in water under stirring for 10 min; (2) H_3PO_4 (85 wt %) was added and the solution stirred for 10 min; (3) HF (48 wt %) was added and the mixture stirred for 1 h; (4) quinuclidine (Q) was added and the gel stirred for a further 1 h; (5) the final gel, with the molar composition $1Ga_2O_3$:$1P_2O_5$:6Q:0.75HF:$64H_2O$, was heated at 150 °C for 24 h in an autoclave with a Teflon liner; (6) the crystalline product was washed with distilled water, dried at 50 °C and stored under ambient conditions. Powder X-ray diffraction (pattern not shown) and ESCA measurements[5] have confirmed that the sample of cloverite was pure and highly crystalline.

Deuteration was carried out in a vacuum line in such a way that only loosely bound intracrystalline H_2O was substituted by D_2O. Bearing in mind the thermal analysis results of ref 3, the sample was dehydrated under high vacuum at 423 K for 5 h. Then ca. 10 wt % of D_2O was adsorbed from the vapor phase at 298 K and the glass ampule with the frozen sample was sealed under vacuum for the ^{2}H → ^{1}H CP experiments.

Solid-state MAS NMR spectra were recorded at room temperature on a Varian VXR-400S WB spectrometer, using a high-speed Doty probe head with 5 mm zirconia rotors driven by dry air at 6−9 kHz. Selected BD spectra were recorded with an ultrahigh speed Doty probe at a MAS rate of 19 kHz. The resonance frequencies for ^{1}H, ^{31}P, ^{71}Ga, and ^{2}H were 400.0, 161.9, 122.0, and 61.4 MHz, respectively. The magic angle was set precisely by observing the ^{79}Br resonance from KBr. The NMR acquisition parameters are given in Table 1.

The conventional single-contact CP pulse sequence with reversal of spin temperature in the rotating frame was used without decoupling during signal acquisition. The ^{1}H → ^{31}P and ^{31}P → ^{1}H CP experiments were set on $NH_4H_2PO_4$, using optimized contact times of 5 and 4 ms, respectively, and a recycle delay of 10 s in both cases. ^{2}H → ^{1}H CP was set on perdeuterated glycine.[20] Variable-contact time CP data were analyzed using the equation:[14]

$$I(t) = A\left(1 + \frac{T_{CP}}{T^{t}_{1\zeta}} - \frac{T_{CP}}{T^{s}_{1\zeta}}\right)^{-1}\left\{\exp\left(\frac{-t}{T^{s}_{1\zeta}}\right) - \exp\left[-t\left(\frac{1}{T_{CP}} + \frac{1}{T^{t}_{1\zeta}}\right)\right]\right\} \quad (1)$$

where $I(t)$ is the intensity of the CP signal, t the contact time, A the amplitude of the signal, T_{CP} the time constant of the CP process, and $T^{s}_{1\zeta}$ and $T^{t}_{1\zeta}$ the spin−lattice relaxation times in the rotating frame for the source and target spins, respectively. Equation 1 is valid for the exact Hartmann−Hahn match and a target/source spin population ratio $\epsilon = 0$.

Relaxation in the laboratory and rotating frames was studied at power levels similar to those for the BD and CP spectra, respectively. For the ^{1}H and ^{31}P resonances, we have measured T_1 by inversion recovery and $T_{1\rho}$ directly using the $(\pi/2)$−SL acquisition pulse sequence (where SL stands for the spin-lock pulse). In addition, we have monitored ^{1}H inversion recovery by ^{1}H → ^{31}P CP using a standard CP pulse sequence preceded in the proton channel by a π pulse and a variable delay. Two-dimensional (2D) ^{1}H spin-diffusion experiments in the rotating frame were performed using the $(\pi/2)-t_1$−SL acquisition (t_2) pulse sequence[27] with 256 increments of t_1 and 16 scans in each, a recycle delay of 2 s, a $\pi/2$ pulse of 5.2 μs duration, and a spin lock at the same power level. The 2D data were processed in both spectral dimensions with sine-bell-shifted apodization and magnitude calculation followed by symmetrization. Conscious of the fact that spin diffusion must be studied using different mixing (spin-lock) times, we have examined the process very carefully. The spin-lock time was varied up to 20 ms. Since all the cross-peaks were present, albeit with different intensities, for the sake of brevity we show only the best spectrum for the spin-lock time of 10 ms.

Results and Discussion

Cloverite Spectra. A ^{1}H NMR spectrum of hydrated cloverite recorded at a MAS rate of 5 kHz was previously discussed by Bedard at al.[3] and is similar to the upper spectrum in our Figure 2. The low-frequency peaks at 3.4 and 2.0 ppm were assigned to α-CH_2 and (β-CH_2 + γ-CH) of the quinuclidinium cation, respectively. The remaining weaker peaks at 7.6 and 6.4 ppm, together with the broad background line, were generally assigned to terminal P−OH and Ga−OH groups with extraframework H_2O. It was assumed that the line from the quinuclidinium proton was completely broadened by the quadrupolar interaction with the quaternary nitrogen and/or exchange effects involving the Brønsted sites and water.

Our ^{1}H BD spectrum recorded under ultrahigh speed MAS is much better resolved (Figure 3). The broad background line, centered at ca. 5 ppm, is less prominent and both template peaks have shoulders. The peak at 8 ppm is clearly broader than that at 6.4 ppm. The latter two peaks disappear upon deuteration and the background is substantially reduced (Figure 2). The background line can be eliminated by a long spin lock, which exposes the peaks at 8 and 6.4 ppm (Figure 2). This is reminiscent of the removal of a peak from mobile water in the ^{1}H spectrum of VPI-5 in order to reveal weak template peaks and a peak at 3.7 ppm from defect P−OH groups.[30]

The ^{31}P BD spectrum of hydrated cloverite was first published by Merrouche et al.[2] Although recorded with MAS at 8 kHz, it was poorly resolved and showed only two lines at −6 and −10 ppm, the former appearing as a shoulder. No specific

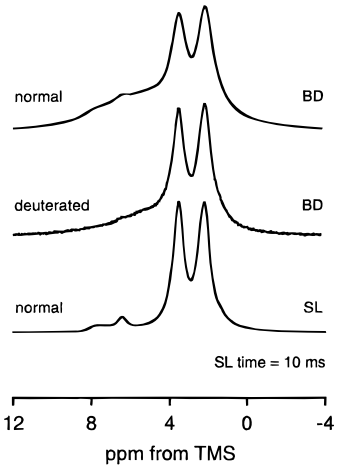

Figure 2. ^{1}H NMR spectra of cloverite. Deuterated cloverite was prepared by substitution of H_2O by D_2O (see Experimental Section). The bottom spectrum was recorded after a spin lock (SL) of the ^{1}H magnetization. The spectra are not shown on the same intensity scale, and only the relative intensities within each spectrum can be compared. Spinning sidebands are outside the spectral region shown.

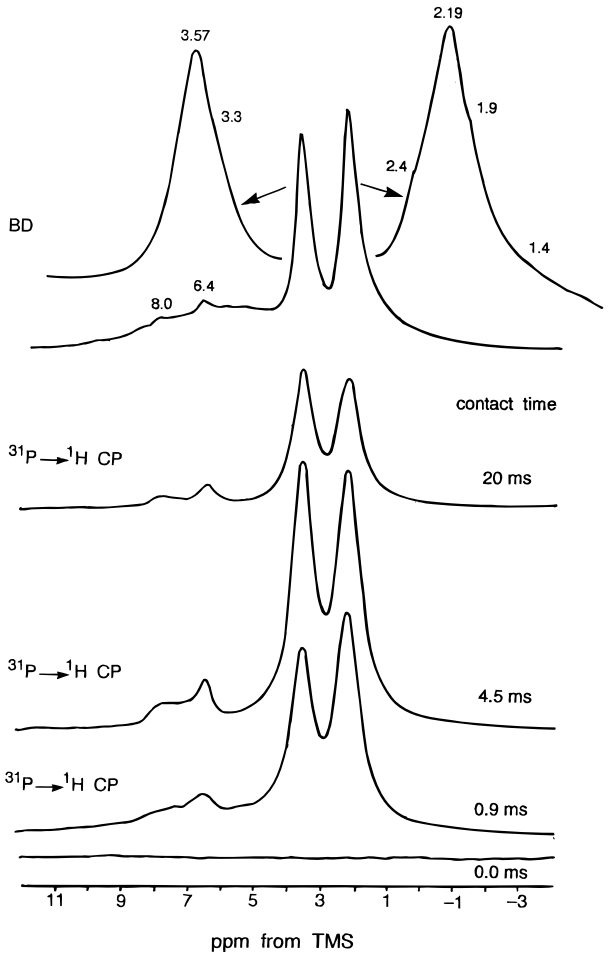

Figure 3. Comparison of the ^{1}H BD and ^{31}P → ^{1}H CP spectra of cloverite recorded with MAS at 19 and 7 kHz, respectively. The CP spectra are on the same intensity scale. Spinning sidebands are outside the spectral region shown.

assignment of the five crystallographic sites was attempted. Better resolved spectra subsequently recorded by several groups[3,5−8] are similar to our spectrum measured with MAS at 19 kHz (Figure 4). However, we have found an extra peak at ca. −14 ppm as a shoulder on the peak at −11 ppm. The ^{31}P spectrum was almost unaffected by deuteration (not shown).

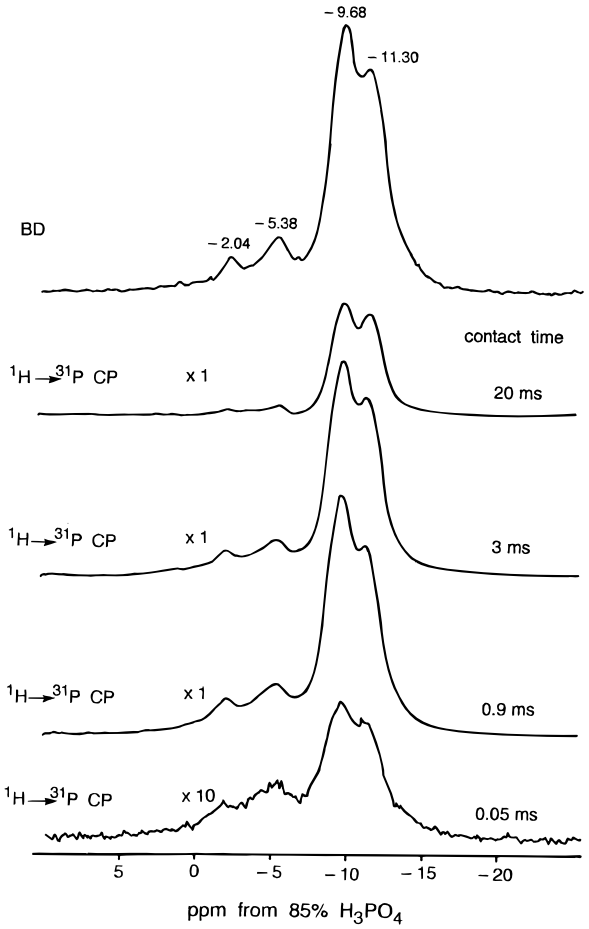

Figure 4. Comparison of the ^{31}P BD and ^{1}H → ^{31}P CP spectra of cloverite recorded with MAS at 19 and 7 kHz, respectively. Note different intensity scaling factors of the CP spectra. Spinning sidebands are outside the spectral region shown.

Bedard et al.[3] compared chemical shifts of cloverite with those of H_3PO_4 and dense-phase metal phosphates. They assigned both the −2 and −5 ppm peaks to sites P3, which bear hydroxyl groups, and the peaks at −10 and −11 ppm to the T-atoms P1, P2, P4, and P5. The comparison of spectral intensity seemed to confirm this assignment. The distribution of the P atoms in the unit cell of cloverite is given by the ratio P1:P2:P3:P4:P5 = 1:0.5:0.5:1:1.[1,3] By integrating the respective peaks, Bedard et al.[3] found that P3:(P1 + P2 + P4 + P5) = 0.5:3.7, very close to the crystallographic ratio of 0.5:3.5. Moreover, the high-frequency part of the ^{31}P spectrum (above −7 ppm) is enhanced by short-contact time CP from protons, which supports the assignment of this spectral region to the $P(OGa)_3OH$ sites (refs 3 and 5 and Figure 4). The peak at −17 ppm, which appeared on dehydration,[3,6] was assigned to P═O groups.[3]

Zibrowius et al.[8] found that the ratio between the sum of the intensities of two high-frequency peaks and the intensities of the peaks at −10 and −11 ppm is ca. 1:5:2, but no details of the deconvolution were given. Such intensity ratio was compatible with the 1:(1:2:2):2 occupancy of the five crystallographic P sites and in agreement with the assignment of both high-frequency peaks to the P−OH groups. Meyer zu Altenschildesche et al.[7] went further in the interpretation and determined number and positions of overlapping ^{31}P peaks using various spectral editing techniques followed by spectral subtraction and deconvolution. To make the task possible, they had to assume five Lorentzian lines with the areas proportional to the occupancy of the crystallographic P sites. The fitted peaks were located at −2.2 (P2 or P3), −5.2 (P2 or P3), −9.6 (P1 or P4),

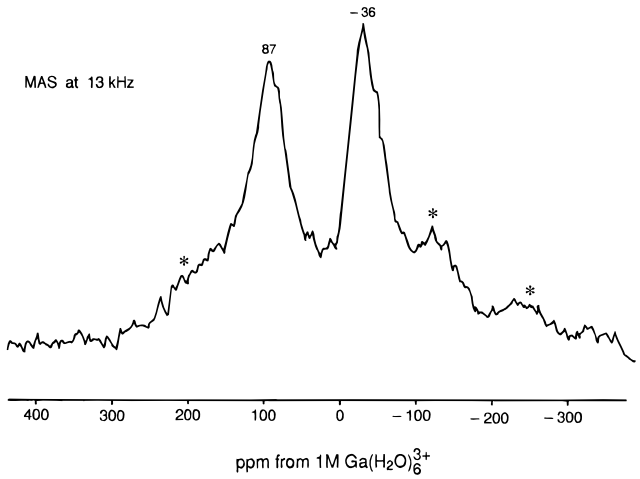

Figure 5. ^{71}Ga NMR spectrum of cloverite. Asterisks denote spinning sidebands.

TABLE 2: Results of the ^{1}H Relaxation Studies in the Rotating Frame[a]

^{1}H peak (ppm)	$T_{1\rho}^{H}$		amplitudes	
	H_A	H_B	H_A	H_B
6.4	0.54 ± 0.08	10.8 ± 0.6	38 ± 5	11.4 ± 0.7
3.6	0.6 ± 0.1	10.7 ± 0.7	70 ± 10	127 ± 5
2.2	0.9 ± 0.2	11 ± 1	65 ± 9	123 ± 7

[a] The $T_{1\rho}^{H}$ relaxation times and the intensity amplitudes are in milliseconds and in arbitrary units, respectively. There are two overlapping ^{1}H NMR patterns, denoted by H_A and H_B. The high-frequency peak lies on top of a broad and intense background band centered at ca. 5 ppm (uppermost spectrum in Figure 2), which gives the dominant contribution to the parameters in the first line of the table.

−10.4 (P5), and −11.6 (P1 or P4) ppm, and the assignment (in parentheses) was conclusive only for the peak at −10.4 ppm. We believe that the general assignment of the ^{31}P peaks above −7 ppm to the $P(OGa)_3OH$ sites and the peaks below −7 ppm to the $P(OGa)_4$ sites is justified. However, arguments based on peak integration or spectral deconvolution are meaningless because the number of the ^{31}P peaks and their relative intensities depend on the degree of hydration of cloverite.

Bradley et al. studied cloverite at various stages of hydration.[6] Dehydrated cloverite gave a peak at −0.8 ppm, assigned to the $P(OGa)_3OH$ sites, and peaks at −10 and −11 ppm, assigned to the $P(OGa)_4$ sites. Upon rehydration, a broad spectral background increased and four new peaks appeared between 0 and −6 ppm. The complex structure of this spectral region was explained by the superposition of the peaks from 29 different $P(OGa)_3OH$ and $P(OGa)_4$ phosphorus atoms with the nearest neighbor Ga atoms at varying degrees of hydration. No specific assignment was made, but it was shown that $^1H \rightarrow {}^{31}P$ CP over a long contact time of 10 ms considerably enhances the high-frequency spectral region. Based on the ^{31}P and ^{71}Ga NMR spectra (Figures 4 and 5) and using the terminology of Bradley et al.,[6] our material should be classified as ambient-humidity cloverite. It contains both five- and six-coordinated Ga, which gives peaks at 87 and −36 ppm, respectively (cf. refs 6 and 7 for the assignment). Each Ga atom is coordinated by a F atom and four or five O atoms. We note that the ^{31}P peaks above −7 ppm are relatively enhanced by short-contact time $^1H \rightarrow {}^{31}P$ CP (refs 3 and 5 and Figure 4), which indicates rather short $^{31}P-{}^1H$ distances possible only within six $P(OGa)_3OH$ sites (Table 2 from ref 6). Instead of six high-frequency peaks, we have detected only two at −2 and −6 ppm (Figure 4) located on a broad background. The model proposed by Bradley et al.[6] thus fails for two possible reasons. First, in hydrated cloverite there is probably proton and water exchange, which shifts peaks and averages them partially or completely. Second, interaction of water with Ga−OH can result in a partial opening of the Ga−O bond at the Ga−O−P bridge[31] followed by a further structural rearrangement.

Relaxation Studies. Detailed rotating-frame spin−lattice relaxation studies reveal that the ^{1}H spectrum of hydrated cloverite is a sum of two separate patterns, each corresponding to a specific single relaxation time $T_{1\rho}^{H}$ (Table 2). We have found the same $T_{1\rho}^{H}$ values of ca. 0.7 and 11 ms for several spectral positions, even those between the peaks, but with different intensity contributions from the two spectral patterns. Broader peaks give a larger contribution to pattern H_A, with short $T_{1\rho}^{H}$, and sharper peaks give a larger contribution to pattern H_B, with long $T_{1\rho}^{H}$. The broad band centered at ca. 5 ppm (uppermost spectrum in Figure 2) belongs therefore almost entirely to pattern H_A, while the template peaks at 3.6 and 2.2 ppm contribute ca. 65% of their intensity to pattern H_B (Table 2). Each template peak presumably consists of a broad background and a sharp component. Such interpretation accounts for the shoulders in the ultrahigh speed MAS spectrum (Figure 3) as well as for the better resolution after a long spin lock (Figure 2), which exposes the H_B pattern.

$T_{1\rho}^{H}$, the relaxation time in the rotating frame, is a volume property. In typical organic solids it is averaged by proton spin diffusion over a distance of ca. 2 nm,[32] thus permitting the identification of different phases in the same sample.[33] It appears therefore that our material contains two types of microdomains, A and B, responsible for spectra H_A and H_B, respectively. Fast spin diffusion within each microdomain averages relaxation times $T_{1\rho}^{H}$ of structurally different protons to a unique value. Microdomains A have short $T_{1\rho}^{H}$ of 0.7 ms and give the ^{1}H spectrum composed of broader peaks. This spectrum contains a huge band centered at 5 ppm (see the inversion−recovery results below), which substantially decreases on substituting H_2O by D_2O (Figure 2) or on dehydration.[3,6] We therefore believe that microdomains A are rich in water and that their $T_{1\rho}^{H}$ value is close to that of extraframework water. Microdomains B have long $T_{1\rho}^{H}$ of 11 ms and give the ^{1}H spectrum composed of sharper peaks, and this spectrum is dominated by the template peaks (Table 2). Microdomains B must have much less water than microdomains A and $T_{1\rho}^{H}$ close to that of template protons.

The concept of two types of microdomains in ambient-humidity cloverite is supported by spin−lattice relaxation studies in the laboratory frame. Both patterns can be discerned near the null point in the conventional ^{1}H inversion recovery experiment (Figure 6a). For the delay of 37.5 ms, pattern H_A is zero while pattern H_B is still inverted. For the delay of 57.5 ms, pattern H_A is predominant while pattern H_B approaches zero. For the delay of 60.0 ms pattern H_B is zero, so one can clearly see the broad band at 5 ppm and the broad components of the template peaks. The broad band at 5 ppm is from various hydroxyl groups: extraframework water, water coordinated to Ga and the P−OH and Ga−OH groups. When isolated, these species give separate peaks but in hydrated cloverite they are probably involved in water and proton exchange mediated by hydrogen bonding. Since extraframework water is abundant, the average chemical shift is close to that of bulk water. For delays longer than 60 ms, the patterns H_A and H_B are positive. A rough null-point estimation gives $T_{1\rho}^{H} = 54$ ms for pattern H_A and $T_{1\rho}^{H} = 87$ ms for pattern H_B. The peak at 1.9 ppm probably comes from the CH group of the quinuclidinium cation.

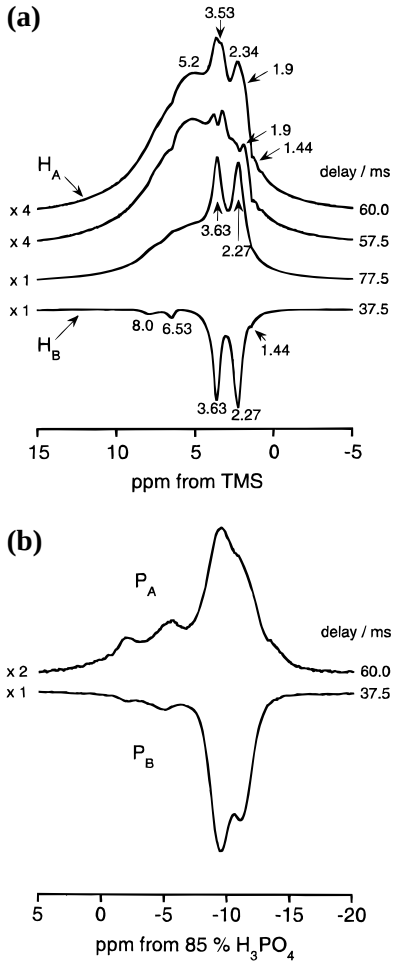

Figure 6. (a) ^{1}H inversion−recovery spectra of cloverite. Note the different intensity scaling factors of the spectra. Spinning sidebands are outside the spectral region shown. (b) ^{1}H inversion recovery monitored by ^{1}H → ^{31}P CP with a contact time of 0.9 ms. The experiment was performed with a standard CP pulse sequence preceded in the proton channel by a π pulse and a variable delay. Note the different intensity scaling factors of the spectra. Spinning sidebands are outside the spectral region shown.

Compared to the chemical shifts of quinuclidinium in D_2O/HF (2.67, 1.51, and 1.30 ppm),[3] the template peaks are shifted by 0.6−0.9 ppm to higher frequency as a result of the confinement of quinuclidinium in cloverite.

The ^{31}P spins in cloverite behave as a single spin system with unique relaxation times $T_{1\rho}^{P} = 35 \pm 2$ ms and $T_{1\rho}^{P} = 6.8 \pm 0.2$ s. However, ^{1}H inversion recovery combined with ^{1}H → ^{31}P cross-polarization shows that microdomains A and B give different ^{31}P spectra, P_A and P_B. For the relaxation delay of 37.5 ms, pattern H_A is zero and pattern H_B nonzero (cf. Figure 6a and the discussion above), so CP proceeds only from protons of microdomains B, giving spectrum P_B (Figure 6b). For the relaxation delay of 60.0 ms the pattern H_B is zero and pattern H_A nonzero (cf. Figure 6a and the discussion above), so CP proceeds only from protons of microdomains A, giving spectrum P_A (Figure 6b). The high-frequency spectral region is relatively more intense in spectrum P_A than in spectrum P_B, indicating a higher content of the P−OH groups in water-rich microdomains A than in water-deficient microdomains B. Moreover, the low-frequency peaks from the $P(OGa)_4$ sites in microdomains A are broader, indicating some structural disorder, and an additional shoulder appears at ca. −14 ppm.

On the basis of elaborate infrared studies, Müller et al.[31] have proposed that interaction of a polar molecule (H_2O, NH_3, or CH_3OH) with Ga−OH may result in a *partial* opening of the Ga−O bond next to the structural hydroxyl group. The Ga site is then converted into a very active catalytic center, which has both Brønsted (Ga−OH) and Lewis (Ga ion) acid properties. We suggest that water can create defect P−OH groups via *complete* hydrolysis:

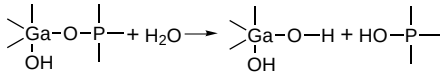

The process locally distorts the crystal lattice and affects the relevant $P(OGa)_4$ sites, the ^{31}P peaks which broaden. The peak at ca. −14 ppm must be related to this structural rearrangement. Müller et al.[31] found that the framework of cloverite collapses upon adsorption of more than one water molecule per Ga−OH group. We believe that this occurs when two Ga−O bonds at the same Ga site are hydrolyzed. If such hydrolysis occurs next to the P3 site, the P atom gains a second hydroxyl group. Such geminal hydroxyl groups can release one molecule of water during dehydration, which would create a P═O group resonating at −17 ppm.[3,6]

CP Kinetics and Spin Diffusion. The presence of the two kinds of microdomains in ambient humidity cloverite is consistent with the ^{1}H → ^{31}P and ^{31}P → ^{1}H CP kinetics. The buildup of the ^{31}P CP peaks is best explained by a sum of two elementary CP functions (eq 1, s = ^{1}H, t = ^{31}P) with the same T_{CP} but different $T_{1\rho}^{H}$ values (Figure 7a). In the case of ^{1}H → ^{31}P CP, the functions are valid for the ^{31}P/^{1}H spin population ratio $\epsilon = 0$. From the unit-cell formula of anhydrous cloverite we obtain $\epsilon = 0.27$. Since the value of ϵ for hydrated cloverite must be much lower, the assumption appears justified. The two fitted $T_{1\rho}^{H}$ values (Table 3) are reasonably close to those obtained directly from the relaxation measurements (Table 2) and assigned to distinct microdomains. The two components of the total kinetic curve for any ^{31}P CP peak must be therefore attributed to the microdomains. The T_{CP} value of 0.4 ms is very short and indicates that CP takes place within the P−OH groups. Other protons, such as those of the template or water coordinated to Ga and the Ga−OH groups, are either too distant from the P sites or belong to mobile extraframework water. Dipolar interactions between these protons and the ^{31}P spins are weak, and thereby, CP is inefficient. For example, in hydrated aluminophosphates VPI-5 and AlPO-H3, ^{1}H → ^{31}P CP proceeds from remote protons of water molecules coordinated to Al, which results in $T_{CP} \geq 1$ ms.[34]

Consider that the $P(OGa)_4$ sites do not participate in the primary CP events but do give the ^{31}P CP peaks, even for the shortest contact times (Figure 4). These sites probably acquire magnetization via ^{31}P spin diffusion from the $P(OGa)_3OH$ sties within the same microdomain. The process occurs simultaneously with CP and must be very fast because it does not affect the kinetics. We note that up to the contact time of 1.5 ms, the kinetics for the $P(OGa)_4$ sites (peaks at −10 and −11 ppm) and the $P(OGa)_3OH$ sites (peaks at −2 and −5 ppm) are governed by the functions of the same type and with the same parameters except for the amplitudes (Figure 7a and Table 3). However, over an induction period of 1.5 ms, slow interdomain spin diffusion in the rotating frame begins to increase the intensities of the peaks at −10 and −11 ppm, while the ^{31}P relaxation in the rotating frame tends to decrease them (Figure 7a). We have assumed that ^{31}P spin diffusion can be roughly described by an exponential function with some average characteristic time constant T_{PP}. The overall process, that is,

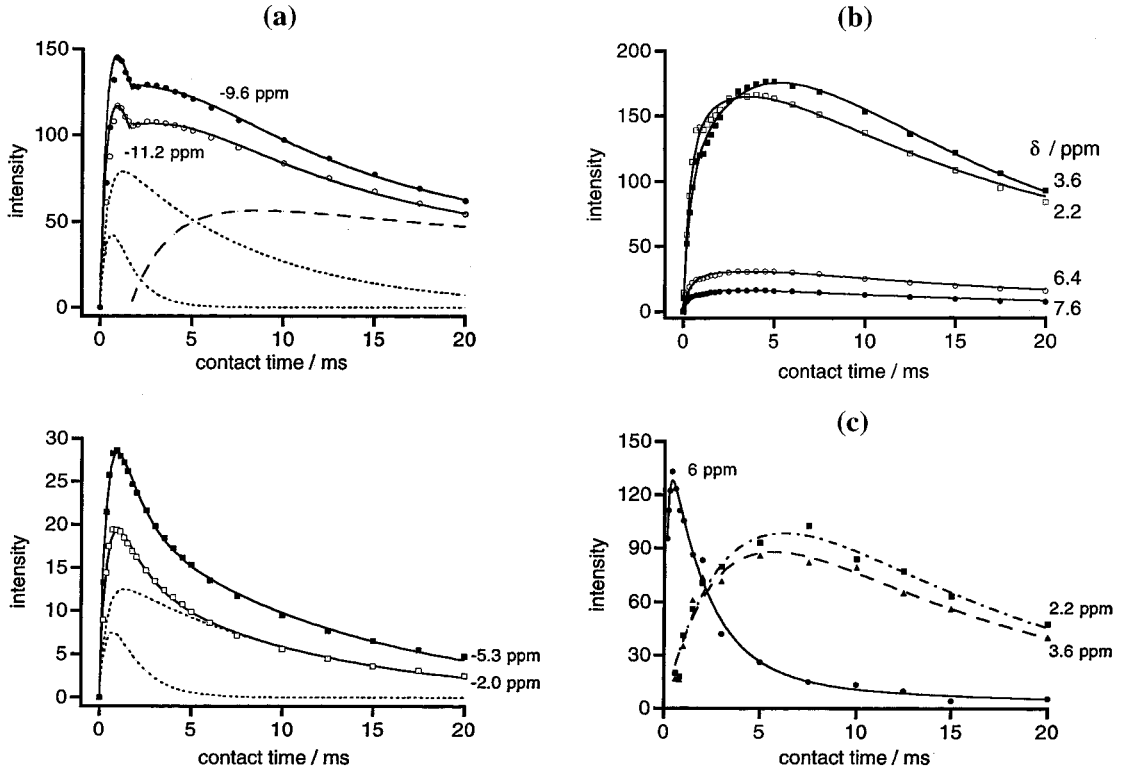

Figure 7. Results of variable-contact time CP experiments with cloverite. (a) $^1H \rightarrow {}^{31}P$ CP experiments. The CP and spin-diffusion components of the kinetic curves are denoted by dotted and broken lines, respectively. The deconvolutions are shown for the peaks at −11.2 and −2.0 ppm. For each curve there are two CP components from two types of microdomains. The peaks at −9.6 and −11.2 ppm have extra contributions from spin diffusion. (b) $^{31}P \rightarrow {}^1H$ CP experiments. (c) $^2H \rightarrow {}^1H$ CP experiment with deuterated cloverite prepared by substitution of H_2O by D_2O (see Experimental Section).

TABLE 3: Fitted Kinetic Parameters of $^1H \rightarrow {}^{31}P$ Cross-Polarization (see Figures 4 and 8)[a]

^{31}P peak (ppm)	$T_{1\rho}^H$		T_{CP}	$T_{1\rho}^D$	T_{PP}	amplitudes		
	P_A	P_B	P_A and P_B			CP (A)	CP (B)	^{31}P spin diffusion
−2.0	1.5 ± 0.4	11 ± 1	0.40 ± 0.03	35 ± 2		16 ± 3	15 ± 1	
−5.4	1.2 ± 0.3	12.2 ± 0.8	0.41 ± 0.04	35 ± 2		27 ± 5	22 ± 1	
−9.7	1.2 ± 0.2	8 ± 1	0.39 ± 0.05	35 ± 1	2.6 ± 0.1	139 ± 9	121 ± 9	86 ± 1
−11.2	1.2 ± 0.2	8 ± 1	0.39 ± 0.05	35 ± 3	2.6 ± 0.1	111 ± 7	97 ± 7	77 ± 3

[a] The $T_{1\rho}^H$ and $T_{1\rho}^P$ relaxation tims, the T_{CP} time constant, and the ^{31}P spin-diffusion time constant T_{PP} are in milliseconds. Amplitudes are in arbitrary units. There are two overlapping ^{31}P NMR patterns denoted by P_A and P_B. The CP kinetics for two high-frequency peaks is described by a sum of two elementary CP functions (eq 1) with the same T_{CP} constant and different $T_{1\rho}^H$ values. For two low-frequency peaks this complex kinetic function was supplemented with the ^{31}P spin-diffusion term (eq 2). The spin diffusion began after an induction period $\tau = 1.50 \pm 0.03$ ms.

spin diffusion accompanied by relaxation, was modeled with a function similar to that for cross-polarization:

$$I(t) = B\left[\exp\left(\frac{-(t-\tau)}{T_{1\rho}^N}\right) - \exp\left(\frac{-(t-\tau)}{T_{NN}}\right)\right] \qquad (2)$$

where N denotes the spin species involved (in this case N = ^{31}P), $I(t)$ is the intensity acquired via spin diffusion, t is the contact time, τ is the induction period (for $t < \tau$ we have $I(t) = 0$), and B is the amplitude intensity, achieveable only without the relaxation. The kinetic function consisting of two CP terms (eq 1) and the spin-diffusion term (eq 2) works reasonably well, since it gives good fittings for the peaks at −10 and −11 ppm from the $P(OGa)_4$ sites (Figure 7a) and provides kinetic parameters consistent with those for the peaks at −2 and −5 ppm from the $P(OGa)_3OH$ sites. However, our simple model cannot predict how the intensity acquired by the particular $P(OGa)_4$ peak via spin diffusion is partitioned between the P_A and P_B patterns. The patterns, defined by the cross-polarization and ^{31}P spin-diffusion amplitudes in Table 3, should ultimately resemble those in Figure 6b.

The intensity of the $^{31}P \rightarrow {}^1H$ CP peaks ought to increase with the time constant $1/(1/T_{CP} + 1/T_{1\rho}^H)$ (eq 1). We know from $^1H \rightarrow {}^{31}P$ CP that T_{CP} is ca. 0.40 ms and that $T_{1\rho}^H$ is ca. 1.3 and 10 ms for microdomains A and B, respectively. Hence, assuming the same T_{CP} value, the respective raising time constants should be 0.31 and 0.39 ms. We found that a single elementary CP function (eq 1) with a mean raising time constant of 0.35 ms is sufficient for quantifying the $^{31}P \rightarrow {}^1H$ CP kinetics (Figure 7b and Table 4). The function has to be supplemented by a spin-diffusion term for the protons (eq 2). Note that CP provides intensity of the template peaks at 3.6 and 2.2 ppm (Figure 3), although the template protons are not involved in the polarization transfer, which occurs within the P−OH groups. This can be only explained by ^1H spin diffusion in the rotating frame, occurring within the P−OH groups at the same time scale as the polarization transfer. For a correct fitting, spin diffusion on all proton sites must be taken into account (Figure 7b and Table 4). This means that the ^1H magnetization is accumulated at some P−OH groups not only by $^{31}P \rightarrow {}^1H$ CP but also by spin diffusion from other proton sites. We attempted to analyze the $^{31}P \rightarrow {}^1H$ CP kinetics in hydrated cloverite using the $^1H/^{31}P$

TABLE 4: Fitted Kinetic Parameters of $^{31}P \rightarrow {}^{1}H$ Cross-Polarization (see Figures 3 and 9)[a]

		amplitudes	
^{1}H peak (ppm)	T_{HH}	CP (A + B)	^{1}H spin diffusion
7.6	2.2 ± 0.4	11.6 ± 0.8	10 ± 2
6.4	2.8 ± 0.4	24 ± 1	21 ± 3
3.6	4.1 ± 0.2	97 ± 3	290 ± 10
2.2	2.8 ± 0.3	128 ± 4	120 ± 10

[a] The ^{1}H spin-diffusion time constants T_{HH} and the intensity amplitudes are in milliseconds and in arbitrary units, respectively. There are two overlapping ^{1}H NMR patterns from microdomains A and B, respectively. The CP kinetics were modeled using a sum of the elementary CP function (eq 1) and a ^{1}H spin-diffusion term (eq 2) assuming $T_{1\rho}^{P} = 35$ ms, $T_{1\rho}^{H} = 10$ ms, $1/T_{CP} + 1/T_{1\rho}^{H} = 1/0.35$ ms^{-1} and $\tau = 0$ (see text).

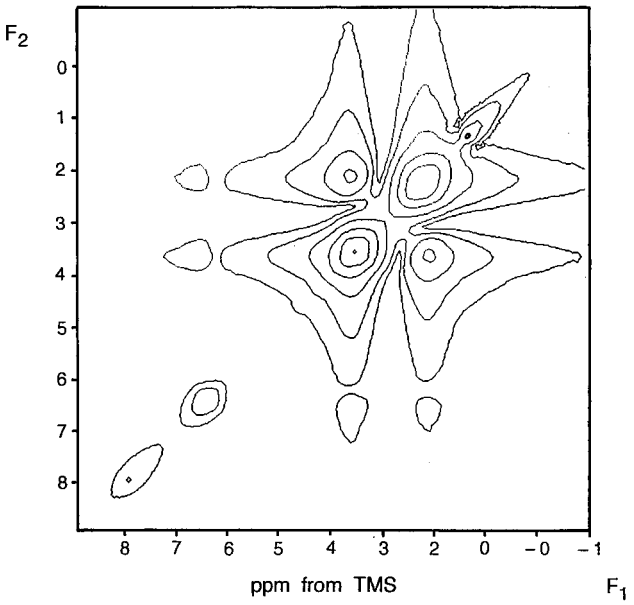

Figure 8. Rotating-frame spin-diffusion ^{1}H spectrum of cloverite.

spin population ratio $\epsilon > 0$, according to the bulk concentrations of H and P, but the results for both $^{1}H \rightarrow {}^{31}P$ and $^{31}P \rightarrow {}^{1}H$ CP were consistent only if we also assumed $\epsilon = 0$ in the latter case. It was not possible to perform fittings using high ϵ values expected from the composition of the hydrated material. We suggest that the parameter ϵ reflects the respective spin-diffusion connectivities established among source spins and among target spins at the moment of the CP contact rather than the bulk ratio of the spin species.

Considering the presence of microdomains and of various types of protons, the ^{1}H spin-diffusion network in hydrated cloverite is clearly very complex. We have tried to use two-dimensional NMR to monitor it directly (Figure 8). Cross-peaks were detected between the template peaks and between each template peak and the sharp peak at 6 ppm. The latter should thus be assigned to P−OH sites because only these sites supply the magnetization to the template protons via spin diffusion. Considering its chemical shift and large line width, the peak at 8 ppm should be assigned to the quinuclidinium proton. We tentatively assign the remaining peak at 1.4 ppm to the Ga−OH groups. All these proton sites are involved in the proton exchange with water, extraframework and associated with Ga, and this exchange shifts and broadens the peaks. P−OH groups from solid surfaces normally resonate below 4 ppm,[35] which means that their Brønsted acidity in cloverite is clearly very high ($\delta = 6.4$ ppm) in accordance with the ESCA and infrared study by Barr et al.[5]

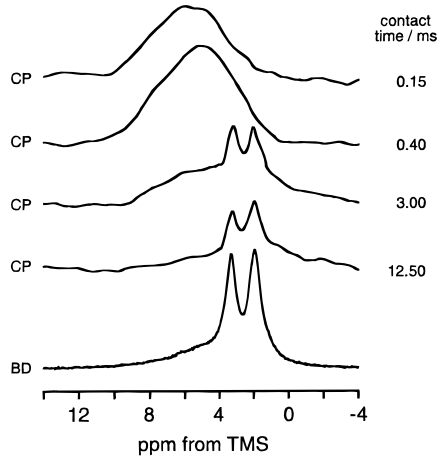

Figure 9. ^{1}H NMR spectra of deuterated cloverite prepared by substitution of H_2O by D_2O (see Experimental Section).

Additional ^{1}H assignments used $^{2}H \rightarrow {}^{1}H$ CP on a sample of cloverite in which H_2O was replaced by D_2O (see Experimental Section). The CP spectra in Figure 9 were recorded from the residual exchangeable protons. We have detected a broad band centered at ca. 6 ppm and dominating the spectra for short contact times and template peaks at 3.6 and 2.2 ppm dominating the spectra for long contact times. The broad band comes from the hydroxyl protons, and its specific assignment is in progress. The large line width of this band can be caused by some exchange process and/or the proximity of a hydroxyl proton to the quadrupolar ^{69}Ga and ^{71}Ga nuclei. Only the quinuclidinium proton in the template can be replaced by deuterium. However, cross-polarization from one quinuclidinium deuterium to 13 alkyl protons of the template seems impossible because of the unfavorable ϵ ratio. Again, ^{1}H spin diffusion was assumed as a mechanism of the magnetization transfer to the template species. The template lines were deconvoluted and the intensities fitted to eq 2 (Figure 7c). We have found $T_{HH} = 2.8 \pm 0.8$ and 3.5 ± 0.8 ms and $T_{1\rho}^{H} = 14 \pm 4$ and 13 ± 3 ms for the peaks at 3.6 and 2.2 ppm, respectively. The $T_{1\rho}^{H}$ values are reasonably close to those in Table 2, so the model used seems to be correct. The results for the broad band were fitted to the elementary CP function (eq 1 and Figure 7c). We found the raising constant $1/(1/T_{CP} + 1/T_{1\rho}^{H}) = 0.14 \pm 0.01$ and $T_{1\rho}^{D} = 2.1 \pm 0.5$. Unfortunately, we were unable to determine $T_{1\rho}^{H}$ separately. Assuming $T_{1\rho}^{H} = 0.54 \pm 0.07$ ms for microdomains A in nondeuterated cloverite, we arrive at $T_{CP} = 0.19 \pm 0.02$ ms. Whatever its exact value, T_{CP} must be very short, which suggests strong $^{2}H-{}^{1}H$ dipolar couplings possible only for short heteronuclear distances in relatively immobile species. Such description fits the HOD molecules coordinated to Ga.

Conclusions

We suggest that ambient-humidity cloverite contains water-rich and water-deficient microdomains. The water-rich regions have faster spin−lattice ^{1}H relaxation and give broader ^{1}H and ^{31}P MAS NMR lines. The overall ^{1}H or ^{31}P spectra consist of two overlapping patterns. The water-rich microdomains contain extra P−OH groups from defect sites probably formed by the hydrolysis of the Ga−O bond at the Ga−O−P bridge next to the hydroxyl group on the Ga atom involved.

The ^{1}H spectrum contains template peaks at 3.6 (α-CH_2), 2.2 (β-CH_2), and 1.9 ppm (CH). The broad weak peak at 8 ppm is from the quinuclidinium protons. The Ga−OH, P−OH, Ga-(H_2O), and extraframework water protons resonate at ca. 1.4, 6.4, 6, and 5 ppm, respectively, and are probably involved in a

mutual proton exchange accompanied by exchange between coordinated and extraframework water. The exchange processes tend to average the chemical shifts and broaden the peaks. Considering the chemical shift, the P−OH groups are unusually acidic.[5] The ^{31}P peaks above −7 ppm come from the $P(OGa)_3$-OH sites and those below −7 ppm from the $P(OGa)_4$ sites.

Cross-polarization between ^{1}H and ^{31}P in hydrated cloverite is reversible. It was found earlier that spin diffusion among the *source* spins affects the CP kinetics.[29,36] We show that spin diffusion between *target* spins with high gyromagnetic ratios, such as ^{1}H and ^{31}P, markedly affects relative intensities of the CP peaks. Detailed analysis of the CP kinetics is very helpful to structural studies and spectral assignments in phosphate molecular sieves.

References and Notes

(1) Estermann, M.; McCusker, L. B.; Bärlocher, C.; Merrouche, A.; Kessler, H. *Nature* **1991**, *352*, 320.

(2) Merrouche, A.; Patarin, J.; Kessler, H.; Soulard, M.; Delmotte, L.; Guth, J. L.; Joly, J. F. *Zeolites* **1992**, *12*, 226.

(3) Bedard, R. L.; Bowes, C. L.; Coombs, N.; Holmes, A. J.; Jiang, T.; Kirkby, S. J.; Macdonald, P. M.; Malek, A. M.; Ozin, G. A.; Petrov, S.; Plavac, N.; Ramik, R. A.; Steele, M. R.; Young, D. *J. Am. Chem. Soc.* **1993**, *115*, 2300.

(4) Huo, Q.; Xu, R.; Li, S.; Ma, Z.; Thomas, J. M.; Jones, R. H.; Chippindale, A. M. *J. Chem. Soc., Chem. Commun.* **1992**, 875.

(5) Barr, T. L.; Klinowski, J.; He, H.; Alberti, K.; Müller, G.; Lercher, J. A. *Nature* **1993**, *365*, 429.

(6) Bradley, S. M.; Howe, R. F.; Hanna, J. V. *Solid State Nucl. Magn. Reson.* **1993**, *2*, 37.

(7) Meyer zu Altenschildesche, H.; Muhr, H.-J.; Nesper, R. *Microporous Mater.* **1993**, *1*, 257.

(8) Zibrowius, B.; Anderson, M. W.; Schmidt, W.; Schüth, F.-F.; Aliev, A. E.; Harris, K. D. M. *Zeolites* **1993**, *13*, 607.

(9) Pines, A.; Gibby, M. G.; Waugh, J. S. *J. Chem. Phys.* **1973**, *59*, 569.

(10) Schaefer, J.; Stejskal, E. O. *J. Am. Chem. Soc.* **1976**, *98*, 1031.

(11) Yannoni, C. S. *Acc. Chem. Res* **1982**, *15*, 201.

(12) Fyfe, C. A. *Solid State NMR for Chemists;* CFC Press: Guelph, Ontario, Canada, 1984.

(13) Mehring, M. *Principles of High-Resolution NMR in Solids*, Springer: Berlin, 1983.

(14) Walter, T. H.; Turner, G. L.; Oldfield, E. *J. Magn. Reson.* **1988**, *76*, 106.

(15) Fyfe, C. A.; Grondey, H.; Mueller, K. T.; Wong-Moon, K. C.; Markus, T. *J. Am. Chem. Soc.* **1992**, *114*, 5876.

(16) Fyfe, C. A.; Mueller, K. T.; Grondey, H.; Wong-Moon, K. C. *J. Phys. Chem.* **1993**, *97*, 13484.

(17) Kolodziejski, W.; Corma, A. *Solid State Nucl. Magn. Reson.* **1994**, *3*, 177.

(18) Kolodziejski, W.; Klinowski, J. *Chem. Phys. Lett.* **1995**, *247*, 507.

(19) Kolodziejski, W.; Corma, A.; Wozniak, K.; Klinowski, J. *J. Phys. Chem.* **1996**, *100*, 7345.

(20) Kolodziejski, W.; Corma, A. *Solid State Nucl. Magn. Reson.*, in press.

(21) Crosby, R. C.; Reese, R. L.; Haw, J. F. *J. Am. Chem. Soc.* **1988**, *110*, 8550.

(22) Abragam, A. *The Principles of Nuclear Magnetism*; Oxford University Press: Oxford, 1961.

(23) Suter, D.; Ernst, R. R. *Phys. Rev.* **1985**, *B32*, 5608.

(24) Szeverenyi, N. M.; Sullivan, M. J.; Maciel, G. E. *J. Magn. Reson.* **1982**, *47*, 462.

(25) Bronnimann, C. E.; Szeverenyi, N. M.; Maciel, G. E. *J. Chem. Phys.* **1983**, *79*, 3694.

(26) Caravatti, P.; Deli, J. A.; Bodenhausen, G.; Ernst, R. R. *J. Am. Chem. Soc.* **1982**, *104*, 5506.

(27) Vega, A. J. *J. Am. Chem. Soc.* **1988**, *110*, 1049.

(28) Kolodziejski, W.; Corma, A.; Barras, J.; Klinowski, J. *J. Phys. Chem.* **1995**, *99*, 3365.

(29) Wu, X.; Zhang, S.; Wu, X. *Phys. Rev.* **1988**, *B37*, 9827.

(30) Kolodziejski, W.; Rocha, J.; He, H.; Klinowski, J. *Appl. Catal.* **1991**, *77*, L1.

(31) Müller, G.; Eder-Mirth, G.; Kessler, H.; Lercher, J. A. *J. Phys. Chem.* **1995**, *99*, 12327.

(32) McBrierty, V. J.; Douglas, D. C. *Macromol. Rev.* **1981**, *16*, 295.

(33) Voelkel, R. *Angew. Chem., Int. Ed. Engl.* **1988**, *27*, 1468.

(34) Blasco, T.; Pérez-Pariente, J.; Kolodziejski, W. *Solid State Nucl. Magn. Reson.*, in press.

(35) Pfeifer, H. *NMR of Solid Surfaces* in *NMR Basic Principles and Progress*; Springer-Verlag: Berlin, 1991; Vol. 31, p 55.

(36) Wu, X.; Zilm, K. W. *J. Magn. Reson.* **1991**, *93*, 265, and references therein.